Aggravation of hepatic ischemia-reperfusion injury with increased inflammatory cell infiltration is associated with the TGF-β/Smad3 signaling pathway

HAIXIA LI[1*], XIAOYUN SHEN[2*], YIFAN TONG[2], TONG JI[2], YAN FENG[3], YANPING TANG[3], RONGYUN MAI[3], JIAXIANG YE[1], TING QUE[1] and XIAOLING LUO[1]

[1]Department of Immunology, School of Basic Medical Sciences, Guangxi Medical University, Nanning, Guangxi 530021; [2]Key Laboratory of Endoscopic Technology Research, Sir Run Run Shaw Hospital, Zhejiang University School of Medicine, Hangzhou, Zhejiang 310016; [3]Research Department, Affiliated Tumor Hospital of Guangxi Medical University, Nanning, Guangxi 530021, P.R. China

Abstract. Ischemia-reperfusion (IR) injury is a major challenge influencing the outcomes of hepatic transplantation. Transforming growth factor-β (TGF-β) and its downstream gene, SMAD family member 3 (Smad3), have been implicated in the pathogenesis of chronic hepatic injuries, such as hepatic fibrosis. Thus, the present study aimed to investigate the role of the TGF-β/Smad3 signaling pathway on hepatic injury induced by IR *in vivo*. In total, 20 129S2/SvPasCrl wild-type (WT) mice were randomized into two groups; 10 mice underwent IR injury surgery and 10 mice were sham-operated. Histopathological changes in liver tissues and serum levels of alanine aminotransferase (ALT) were examined to confirm hepatic injury caused by IR surgery. The expression levels of TGF-β1, Smad3 and phosphorylated-Smad3 (p-Smad3) were detected via western blotting. Furthermore, a total of five Smad3$^{-/-}$ 129S2/SvPasCrl mice (Smad3$^{-/-}$ mice) and 10 Smad3$^{+/+}$ littermates received IR surgery, while another five Smad3$^{-/-}$ mice and 10 Smad3$^{+/+}$ littermates received the sham operation. Histopathological changes in liver tissues and serum levels of ALT were then compared between the groups. Furthermore, hepatic apoptosis and inflammatory cell infiltration after IR were evaluated in the liver tissues of Smad3$^{-/-}$ mice and Smad3$^{+/+}$ mice. The results demonstrated that the expression levels of TGF-β1, Smad3 and p-Smad3 were elevated in hepatic tissue from WT mice after IR injury.

Aggravated hepatic injury, increased apoptosis and enhanced inflammatory cell infiltration induced by hepatic IR injury were observed in the Smad3$^{-/-}$ mice compared with in Smad3$^{+/+}$ mice. Collectively, the current findings suggested that activation of the TGF-β/Smad3 signaling pathway was present alongside the hepatic injury induced by IR. However, the TGF-β/Smad3 signaling pathway may have an effect on protecting against liver tissue damage caused by IR injury *in vivo*.

Introduction

Hepatic ischemia-reperfusion (IR) injury is a common complication that occurs due to a variety of factors, such as liver transplantation, shock and trauma (1). Temporary blood flow deprivation (ischemia) and restoration (reperfusion) of the organs are the primary pathological processes occurring in IR (2). Liver parenchymal cell death is caused by ischemic injury, which involves metabolic disorders and oxidative stress. Moreover, inflammatory mediators cause further damage during blood reperfusion (3). In addition, hepatic IR injury affects the quality of donor livers and the prognosis of liver transplantation (4).

The transforming growth factor-β (TGF-β) superfamily exerts multiple biological functions via the secretion of inhibins, activins and bone morphogenetic proteins (BMPs), which are involved in regulating a range of biological processes, for example BMPs can induce endochondral bone formation (5-7). TGF-β is an important activated mediator of myofibroblasts, which activates stellate cells to secrete collagen fibers, in turn leading to liver fibrosis (8,9). The abnormal expression of TGF-β not only promotes the proliferation and migration of liver cancer cells, but it is also associated with viral hepatitis, hepatic failure and other chronic hepatic diseases (10-14). As the downstream effector of TGF-β, SMAD family member 3 (Smad3) activation is induced by its phosphorylation to phosphorylated-Smad3 (p-Smad3) and the signal is transported to the nucleus, thus forming the classic TGF-β/Smad3 signal transduction pathway (15). The Smad3 linker region can be phosphorylated by intracellular kinases and affects TGF-β responses, such as tumor growth inhibition (16).

A previous study reported that the TGF-β/Smad3 signaling pathway was activated and promoted ventricular remodeling after IR injury in rats (17), while mediating the protection of myocardial cells against IR injury via the stimulation of sphingosine-1-phosphate (S1P)/S1P receptor 1. TGF-β1/Smad3 has also been reported to exert an important effect on cerebral ischemia. For example, Smad3 has been shown to exhibit neuro-protective effects on the brain following IR via the induction of anti-inflammatory and anti-apoptotic pathways (18). Thus, it was hypothesized that the TGF-β1/Smad3 signaling pathway may be able to protect liver cells from IR injury. Therefore, the present study investigated the role of TGF-β/Smad3 in achieving clinical transformation in IR-induced acute liver injury and provide a novel therapeutic target for the prognosis of liver surgery.

Materials and methods

Animals. In total, 20 129S2/SvPasCrl wild-type (WT) mice, aged 6-8 weeks and weighing 22-25 g, were purchased from the Laboratory Animal Center of Zhejiang University School of Medicine (Hangzhou, China) and were random-ized into sham-operated (SH-WT) and IR injury (IR-WT) groups (n=10/group). A total of four Smad3$^{+/-}$ heterozygous 129S2/SvPasCrl mice were donated by The Second Military Medical University (Shanghai, China). Mating of Smad3$^{+/-}$ mice was followed by sibling mating of offspring-generated Smad3$^{+/-}$ mice, to obtain Smad3$^{+/+}$ mice and Smad3$^{-/-}$ mice for experiments. The mouse genotypes were identified at 3 weeks of age, and DNA was isolated from the toes of mice by heating to 100°C with 50 mM NaOH for 10 min. Then, 2X Phanta Max Master Mix (cat. no. P515-01; Vazyme Biotech Co., Ltd.) was used for PCR amplification. The amplification conditions were set as follows: Initial denaturation at 95°C for 3 min, followed by 35 cycles at 95°C for 15 sec, 59°C for 15 sec and 72°C for 30 sec. Then, 3% Tris-acetate-EDTA buffer agarose gel electrophoresis was used to identify the Smad3 gene-deficient mouse genotype, and visualized under the ChemiDoc™ System (cat. no. 1708265; Bio-Rad Laboratories, Inc.). The primers used for genotyping are listed in Table I. The overall morphology of Smad3 mice was assessed and homozygous Smad3$^{-/-}$ mutant (MUT) mice were found to be smaller than littermate Smad3$^{+/-}$ and Smad3$^{+/+}$ mice. Then, the mice were divided into four groups: Smad3$^{+/+}$ mice that underwent a sham operation (SH-WT; n=10); Smad3$^{+/+}$ mice with IR liver injury (IR-WT; n=10); Smad3$^{-/-}$ mice that underwent a sham operation (SH-MUT; n=5); and Smad3$^{-/-}$ mice with IR liver injury (IR-MUT; n=5).

All mice were maintained on a 12/12-h light/dark cycle under controlled humidity (50±10%) and temperature (25±0.5°C) in a specific pathogen-free environment and allowed free access to standard chow and water in the Experimental Animal Center of Sir Run Run Shaw Hospital, Zhejiang University School of Medicine. All animal experiments included in this protocol adhere to the Animal Research: Reporting *In Vivo* Experiments guidelines (19), and were approved by the Animal Testing Ethics Committee of Sir Run Run Shaw Hospital, Zhejiang University School of Medicine (approval no. 20171120-14).

Model of IR liver injury. The present study used a non-lethal segmental (70%) liver IR model as previously described (20).

In brief, a vertical incision was made to each layer to expose the liver after the mouse was anesthetized (4% chloral hydrate sodium; 400 mg/kg) by intraperitoneal injection. The blood vessels, except those of the caudate and right lobes, were occluded with the vascular clamp for 30 min to block the blood flow without injuring the remaining liver tissues. Subsequently, the vascular clamp was gently removed and the blood flow and liver tissues were assessed without injuring before the wound was sutured. In the sham group, surgery was performed by exposing the blood vessels only for 30 min without blocking. Subsequently, recipient animals were intraperitoneally injected with anesthesia (4% chloral hydrate sodium; 400 mg/kg) at the end of the predetermined period (after 6 h of reperfusion), and then the blood samples were collected from the orbital venous plexus to assess serum alanine aminotransferase (ALT) levels. Mice were then sacrificed by cervical dislocation, and the death of mice was confirmed when the respiration and various reflexes had ceased. A portion of the IR injury tissue was used for extraction and detection of total protein and RNA. Then, ~1.0x1.0x1.0-cm liver tissues were promptly fixed overnight in 4% paraformaldehyde (cat. no. 6148; Sigma-Aldrich; Merck KGaA) at room temperature.

Histopathological evaluation. The hepatic tissues were fixed in 4% paraformaldehyde for 8 h at room temperature, dehy-drated, embedded in paraffin, sectioned to 3-μm thickness, stained with hematoxylin for 3 min, rinsed under running water for 5 min, stained with eosin for 2 min and sealed at room temperature. Stained tissues were viewed and imaged using a light microscope. The Suzuki histological grading scores for liver damage were determined as described previously (21). A score of 0 indicated minimal or no evidence of damage, 1 indicated mild damage with cytoplasmic vacuolation and interstitial disorder, 2 indicated moderate to severe damage with extensive nuclear pyknosis and interstitial congestion, and 3 indicated serious necrosis with disintegration of liver cells, hemorrhage and inflammatory cell infiltration.

Detection of ALT levels. Blood samples were centrifuged at 4°C for 5 min at 1,500 x g after standing for 1 h at room temperature and the serum was separated. Serum levels of ALT were determined using an ALT Assay kit (cat. no. C009-2-1; Nanjing Jiancheng Biological Technology), according to the manufacturer's instructions.

Reverse transcription-quantitative PCR (RT-qPCR). The fresh hepatic tissue was homogenized using an automatic sample quick grinding machine (model JXFSTPRP-24; Shanghai Jingxin Industrial Development Co., Ltd.). Total RNA was extracted using TRIzol® reagent (cat. no. 10296-028; Invitrogen; Thermo Fisher Scientific, Inc.) according to the manufacturer's instructions. cDNA was synthesized from RNA using the Hifair® II 1st Strand cDNA Synthesis SuperMix for RT (cat. no. 11121ES60; Shanghai Yeasen Biotechnology Co., Ltd.). The temperature conditions reverse transcription were as follows: 42°C for 15 min and 85°C for 2 min. qPCR was performed using the FastStart Universal SYBR Green Master (ROX) mix (cat. no. 04913914001; Roche Diagnostics), according to the manufacturer's instructions. The amplification conditions were set as: Initial denaturation at 95°C for 10 min, followed by 40 cycles at 95°C for 15 sec, 60°C for

Table I. Primers used for genotyping and reverse transcription-quantitative PCR.

Target gene	Forward primer (5'→3')	Reverse primer (5'→3')
Smad3 WT/MUT	CCACTTCATTGCCATATGCCCTG	
Smad3 WT	CCCGAACAGTTGGATTCACACA	
Smad3 MUT	CCAGACTGCCTTGGGAAAAGC	
β-actin	GGCTGTATTCCCCTCCATCG	CCAGTTGGTAACAATGCCATGT
TLR4	ATGGCATGGCTTACACCACC	GAGGCCAATTTTGTCTCCACA
IFN-γ	AGGTCAACAACCCACAGGTC	ATCAGCAGCGACTCCTTTTC
TNF	TAGCTCCCAGAAAAGCAAGC	TTTTCTGGAGGGAGATGTGG
B220	GTTTTCGCTACATGACTGCACA	AGGTTGTCCAACTGACATCTTTC
CD3E	ATGCGGTGGAACACTTTCTGG	GCACGTCAACTCTACACTGGT
Ly-6G	CGCCCCACTACTCTGGACAATAC	AAACCAGGCTGAACAGAAGCACCC

MUT, mutant; WT, wild-type; Smad3, SMAD family member 3; TLR4, Toll-like receptor 4; Ly-6G, lymphocyte antigen 6 complex locus G6D.

1 min and 60˚C for 30 sec. TsingKe Biological Technology synthesized the primers for PCR (Table I). The $2^{-\Delta\Delta Cq}$ method was used to analyze the data (22).

Western blotting. RIPA lysis buffer (Beyotime Institute of Biotechnology), supplemented with protease inhibitor cocktail (cat. no. HY-K0011; MedChemExpress) and phosphatase inhibitor cocktail (cat. no. HY-K0022; MedChemExpress), was used to extract total proteins. Liver tissues were homogenized in protein lysis buffer on ice and the protein concentrations were measured using a BCA protein assay kit (cat. no. CW0014; CoWin Biosciences). The proteins (20 μg) were loaded onto each lane and separated via 15% SDS-PAGE, and then transferred onto a PVDF membrane (cat. no. IPVH00010; MilliporeSigma). Then, 5% skimmed milk (BD Biosciences) was used to block the membrane for 1 h using a rocking shaker at room temperature; then, the membranes were incubated for 8 h, at a minimum temperature of 4˚C, with primary antibodies against Smad3 (1:1,000; cat. no. ab208182; Abcam), p-Smad3 (1:500; cat. no. bs-3425R; BIOSS), TGF-β1 (1:1,000; cat. no. ab215715; Abcam), β-actin (1:1,000; cat. no. 20536-1-AP; ProteinTech Group, Inc.) and cleaved caspase-3 (1:2,000; cat. no. ab214430; Abcam). The following day, the membrane was thoroughly rinsed three times in western blot washing buffer (cat. no. CW0043S; CoWin Biosciences), followed by incubation with an appropriate HRP-conjugated secondary antibody (1:4,000; cat. no. FDR007; Fdbio Science) for 1 h at room temperature. Finally, ECL reagents (cat. no. FD8030; Fdbio Science) were used to assess the antigen-antibody complex on the membrane. The bands were detected using the ChemiDoc™ Touch Imager (Bio-Rad Laboratories, Inc.) and analysis was performed using ImageLab software version 5.2 (Bio-Rad Laboratories, Inc.). The ratio of phosphorylated protein/total protein was evaluated by ImageJ version 1.0 software (National Institutes of Health).

Immunohistochemistry. The hepatic tissues were fixed in 4% paraformaldehyde for 8 h at room temperature, fixed tissue was processed using an autoprocessor machine (cat. no. ASP200S; Leica Microsystems GmbH), and then the tissues were cut into 3-μm sections and the antigen retrieval process was performed in sodium citrate solution (cat. no. C1010; Beijing Solarbio Science & Technology Co., Ltd.) in a high-pressure steam boiler for 10 min, followed by incubation with 3% H_2O_2 for 15 min at room temperature and blocking with 10% goat serum (cat. no. G9023; Sigma-Aldrich; Merck KGaA) in PBS for 1 h. Slides were incubated with primary antibodies against CD45 (1:250; cat. no. 14-0454-85; eBioscience; Thermo Fisher Scientific, Inc.), Ki67 (1:10,000; cat. no. ab15580; Abcam) or F4/80 (1:250; cat. no. 4339486; Invitrogen; Thermo Fisher Scientific, Inc.) at 4˚C overnight. Next, the slides were restored to normal temperature and washed with PBS three times and then processed using the GTvision immunohistochemical kit (cat. no. GK600710; Shanghai, Gene Tech Company Ltd.) according to the manufacturer's instructions. Slides were incubated with anti-mouse/rabbit secondary antibodies, included in the aforementioned kit, at room temperature for 30 min from the working solution B of the kit, the DAB solution was prepared according to the kit instructions and the reaction time was controlled under the light microscope. After counterstaining with hematoxylin (same procedure as aforementioned), it was sealed with neutral resin (cat. no. MB0722; Dalian Meilun Biology Technology Co., Ltd.). Stained tissues were viewed and imaged under a light microscope.

TUNEL staining. The hepatic tissues were fixed in 4% paraformaldehyde for 8 h at room temperature, fixed tissue was processed using an autoprocessor machine, and then the tissues were cut into 3-μm sections. Hepatocyte apoptosis in paraffin-embedded sections was determined with the TUNEL kit (cat. no. KGA703; Nanjing KeyGen Biotech Co., Ltd.) according to the manufacturer's instructions, as previously described (20). After staining the nuclei with hematoxylin (same procedure as aforementioned), it was sealed with neutral resin. Stained tissues were viewed and imaged using a light microscope (23).

Statistical analysis. GraphPad Prism 8.00 software (GraphPad Software, Inc.) was used for all statistical analyses. Data are presented as the mean ± SEM of a minimum of three independent experiments. Differences among multiple groups were
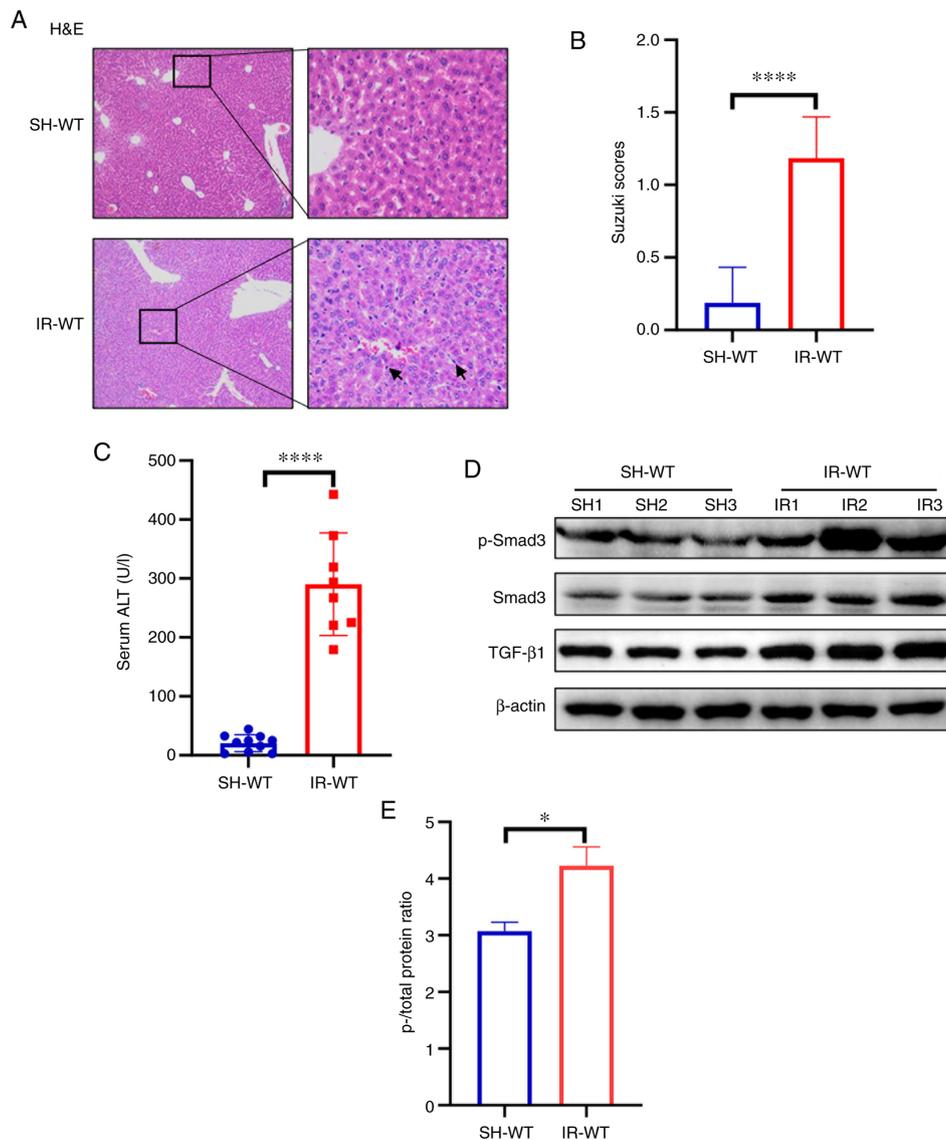
Figure 1. TGF-β1/Smad3 signaling is activated during hepatic IR injury in 129S2/SvPasCrl WT mice. (A) Liver pathological changes were analyzed via histopathological evaluation in hepatic IR injury tissue (magnification, x100 and x400). The black arrows indicate the positive inflammatory cells. (B) Suzuki injury score from H&E staining. (C) Levels of the transaminase ALT were detected in serum samples from the IR-WT and SH-WT groups. (D) Protein expression levels of TGF-β1, Smad3 and p-Smad3 were determined in hepatic tissues by western blotting. SH1, SH2 and SH3 indicate three randomly selected samples from the SH-WT group. IR1, IR2 and IR3 indicate three randomly selected samples from the IR-WT group. (E) ImageJ software was used to perform grayscale analysis, to evaluate the ratio of p- vs. total protein. β-actin was used as the internal reference. *P<0.05, ****P<0.0001. IR-WT, IR injury in 129S2/SvPasCrl WT mice (n=10); SH-WT, sham operation in 129S2/SvPasCrl WT mice (n=10). ALT, alanine aminotransferase; IR, ischemia-reperfusion; p-, phosphorylated; Smad3, SMAD family member 3; TGF-β1, transforming growth factor-β1; WT, wild-type.

analyzed using one-way ANOVA followed by Tukey's post hoc test. Ordinal data were analyzed using non-parametric tests, Mann-Whitney U or Kruskal-Wallis followed by Dunn's post hoc test. Data were analyzed using SPSS version 17.0 (SPSS, Inc.). P<0.05 was considered to indicate a statistically significant difference.

Results

TGF-β1/Smad3 signaling is activated during hepatic IR injury in 129S2/SvPasCrl WT mice. Firstly, the hepatic IR injury model was established in mice. Subsequently, serum ALT levels were determined and H&E staining was performed. As presented in Fig. 1A, the hepatic cells were arranged in neat rows and the lobular structure in the SH-WT group was

still clear; however, the swelling and mild vacuolation in the IR-WT group contrasted with that seen in the SH-WT group. Moreover, the Suzuki histological grading value was significantly increased following liver IR injury in the IR-WT group compared with that in the SH-WT group (Fig. 1B). It was revealed that the levels of ALT were significantly increased in the hepatic IR injury group compared with those in the SH-WT group (Fig. 1C). These results indicated hepatocellular damage occurred and confirmed that the mouse model of liver IR injury had been successfully established.

Furthermore, the expression levels of TGF-β1, Smad3 and p-Smad3 were increased in the hepatic tissue homogenates of mice in the IR-WT group compared with those in the SH-WT group (Fig. 1D). ImageJ software was used to perform grayscale analysis; the ratio of p- and total protein indicated
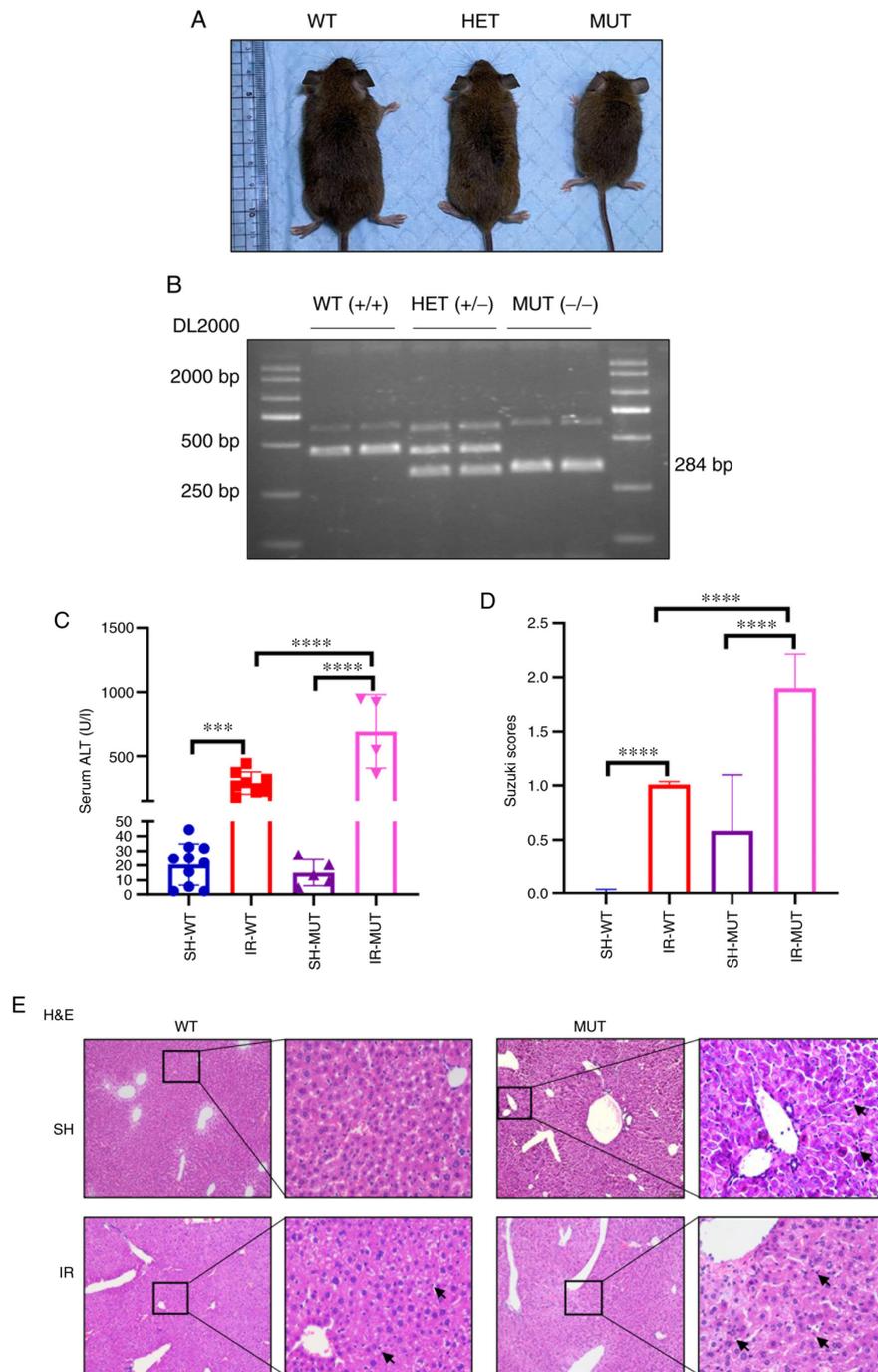
Figure 2. Aggravated hepatic IR injury in Smad3^{-/-} mice. (A) Smad3^{-/-} MUT mice appeared smaller than littermate WT mice or HET mice. (B) Genotyping was performed via agarose gel electrophoresis. The 431 bp band is the WT transcript and the 284 bp band is the MUT transcript. (C) Levels of serum ALT were detected. (D) Suzuki injury score from H&E staining. (E) Liver pathological changes were analyzed via histopathological evaluation in hepatic tissue (magnification, x100 and x400). The black arrows indicate the positive inflammatory cells. [***]P<0.001, [****]P<0.0001. IR-WT, IR injury in Smad3 WT mice (n=10); SH-WT, sham operation in Smad3 WT mice (n=10); IR-MUT, IR injury in Smad3 MUT mice (n=5); SH-MUT, sham operation in Smad3 MUT mice (n=5). ALT, alanine aminotransferase; HET, heterozygote; IR, ischemia-reperfusion; MUT, mutant; Smad3, SMAD family member 3; WT, wild-type.

that p-Smad3 protein expression was significantly increased in the IR-WT group compared with the SH-WT group (Fig. 1E). These results suggested that the TGF-β/Smad3 signaling pathway was activated during liver IR injury in mice.

Aggravated hepatic IR injury in Smad3 gene-deficient mice. To determine the effect of the TGF-β/Smad3 signaling pathway on the induction of hepatic IR damage in mice, Smad3 gene-deficient mice were prepared in order to block the TGF-β1/Smad3

signaling pathway. The Smad3 gene was expressed during embryonic development (24), Smad3 expression was detected in adult Smad3^{-/-} mice liver tissues (data not shown). There was no obvious phenotypic difference between the Smad3^{+/+} and Smad3^{+/-} heterozygous littermates, whereas 70% of the Smad3^{-/-} mice were smaller prior to weaning (Fig. 2A). The PCR analysis revealed a small fragment of 284 bp in Smad3^{-/-} mice, and a large fragment of 431 bp in the Smad3^{+/+} mice, which confirmed the genotype of the mice (Fig. 2B).

To further identify which component served an important role in the mouse liver following IR injury, the current study investigated whether TGF-β/Smad3 possessed a protective effect. The results indicated that the levels of serum ALT were increased in the IR-MUT group compared with those in the SH-MUT, SH-WT and IR-WT groups (Fig. 2C). The pathological changes after liver injury in the IR-MUT group were more notable than in the IR-WT group, these changes included swelling, mild vacuolation and hepatic sinus hyperemia (Fig. 2E). In addition, the Suzuki histological grading score was significantly higher in the IR-MUT group compared with that in the IR-WT group (Fig. 2D).

Apoptosis is increased in Smad3 gene-deficient mice following liver IR injury. To further examine the hepatic cell apoptosis and proliferation in Smad3$^{-/-}$ mice following liver IR injury, TUNEL and Ki67 staining assays were conducted. The expression levels of cleaved caspase-3 were detected via western blotting, and caspase-3 expression levels were measured using immunohistochemistry. Elevated expression of cleaved caspase-3 was detected in the IR-MUT group compared with IR-WT group (Fig. 3A). Furthermore, increased staining of caspase-3-positive hepatocytes was found in the hepatic lobule portal area of the IR-MUT group compared with that in the IR-WT group (Fig. 3B). It was also identified that the staining of TUNEL-positive hepatocytes was increased in the IR-MUT mice compared with that in the IR-WT group (Fig. 3C). Although a high level of proliferation was observed in both the IR groups in comparison with that in the sham-operated mice, no differences were observed between the IR-WT and IR-MUT groups based on Ki67 staining results (Fig. 3D). These findings demonstrated that Smad3 gene deficiency may aggravate liver IR damage by promoting hepatocyte apoptosis in mice.

Inflammatory cell infiltration in Smad3 gene-deficient mice following liver IR injury. IR not only causes damage to liver parenchymal cells, but also causes the infiltration of inflammatory cells and the secretion of inflammatory factors (25). To further examine the possible mechanism via which Smad3 knockout could aggravate liver injury, inflammatory cells, including inflammatory neutrophils [lymphocyte antigen 6 complex locus G6D (Ly-6G)], leukocyte infiltration (CD3) and macrophage cells (F4/80) were analyzed. The results revealed increased staining of CD45- (Fig. 4A) and F4/80-positive (Fig. 4B) cells in the hepatic tissues of the IR-MUT group compared with that in the IR-WT group.

To further verify the inflammatory cell infiltration in Smad3$^{-/-}$ mice following liver IR injury, the mRNA expression levels of B220, CD3E and Ly-6G were assessed. The results indicated that the mRNA expression levels of Ly-6G were significantly increased, whereas B220 mRNA expression levels were decreased in the hepatic tissue homogenates of the IR-MUT group compared with those in the IR-WT group; and there was no significant difference in CD3E mRNA expression (Fig. 4C). Additionally, it was observed that Toll-like receptor (TLR)4, TNF and IFN-γ mRNA expression levels were significantly increased in the IR-WT group compared with SH-WT groups; and TLR4, TNF and IFN-γ mRNA expression levels were significantly increased in the SH-MUT group compared with SH-WT groups; however, the opposite result was observed in Smad3$^{-/-}$ mice, in which the expression levels of TLR4, IFN-γ and TNF mRNA in the IR-MUT group were decreased compared with the SH-MUT group (Fig. 4D). These results suggested that the TGF-β/Smad3 signaling pathway may directly or indirectly regulate the TLR4 signaling pathway. These findings demonstrated that inflammatory cell infiltration was significantly aggravated in Smad3 gene-deficient mice following liver IR injury.

Discussion

IR injury in the liver is one of the most severe side effects of liver surgery and transplantation, and is also the main factor affecting the quality of the transplanted liver (24). Tissue IR injury can occur during organ harvesting and peri-transplantation. It has been shown that microcirculatory dysfunction and immune adjustment are associated with the pathogenesis of liver IR damage (26,27). Previous studies have reported that neutrophil inflammatory cells were detected following IR injury in the liver (28-30). In conditions such as ischemia, hypoxia and IR liver injury, a large number of oxygen free radicals can be produced, which induce the oxidative stress response and liver damage (31). The present study demonstrated that the TGF-β/Smad3 signaling pathway was activated after liver IR injury in a mouse model of liver IR and revealed that TGF-β/Smad3 signaling pathway activation may serve a role in protection of hepatic cells, as the attenuation of this pathway caused aggravated hepatic cell injury.

TGF-β1 is one of three isoforms of the TGF-β superfamily (32). TGF-β/Smad3 has been revealed to be associated with IR injury in several organs. For example, the interaction of Wnt/β-catenin and TGF-β/Smad signaling pathways was shown to exert neuroprotective effect in rats with cerebral IR injury (33). Moreover, in a previous study, microRNA-211 suppressed apoptosis and relieved kidney injury following IR by targeting the TGF-β/Smad3 signaling pathway (34). It has also been shown that TGF-β1 may contribute to isoflurane post-conditioning against cerebral IR injury by inhibiting the JNK signaling pathway (35). In the present study, it was demonstrated that TGF-β1 was more highly expressed in hepatic tissue derived from mice with liver IR injury compared with that in the sham-operated group.

Considering that TGF-β is the strongest fibrotic factor and pro-inflammatory factor, which can also aggravate IR injury (36), the present study aimed to reduce the effect of IR injury by blocking TGF-β/Smad signaling. As homozygous TGF-β1 (37,38) and Smad2 mutations in mice were all embryonic lethal (39,40), the current study selected Smad3 gene-deficient mice (41,42) as a model for further examination. This strain of Smad3 MUT mice was reported to have deficient TGF-β signaling, and studies using the TGF-β responsive reporter 3TP-Lux failed to show any activation by the MUT construct (24,42), which indicated that TGF-β signaling was attenuated in these mice. However, the present results indicated that IR injury was more severe in Smad3 gene-deficient mice, with increased hepatocyte apoptosis and higher inflammatory cell infiltration. The results showed that endogenous deletion of the TGF-β/Smad3 signaling pathway could aggravate IR injury, which indirectly demonstrated
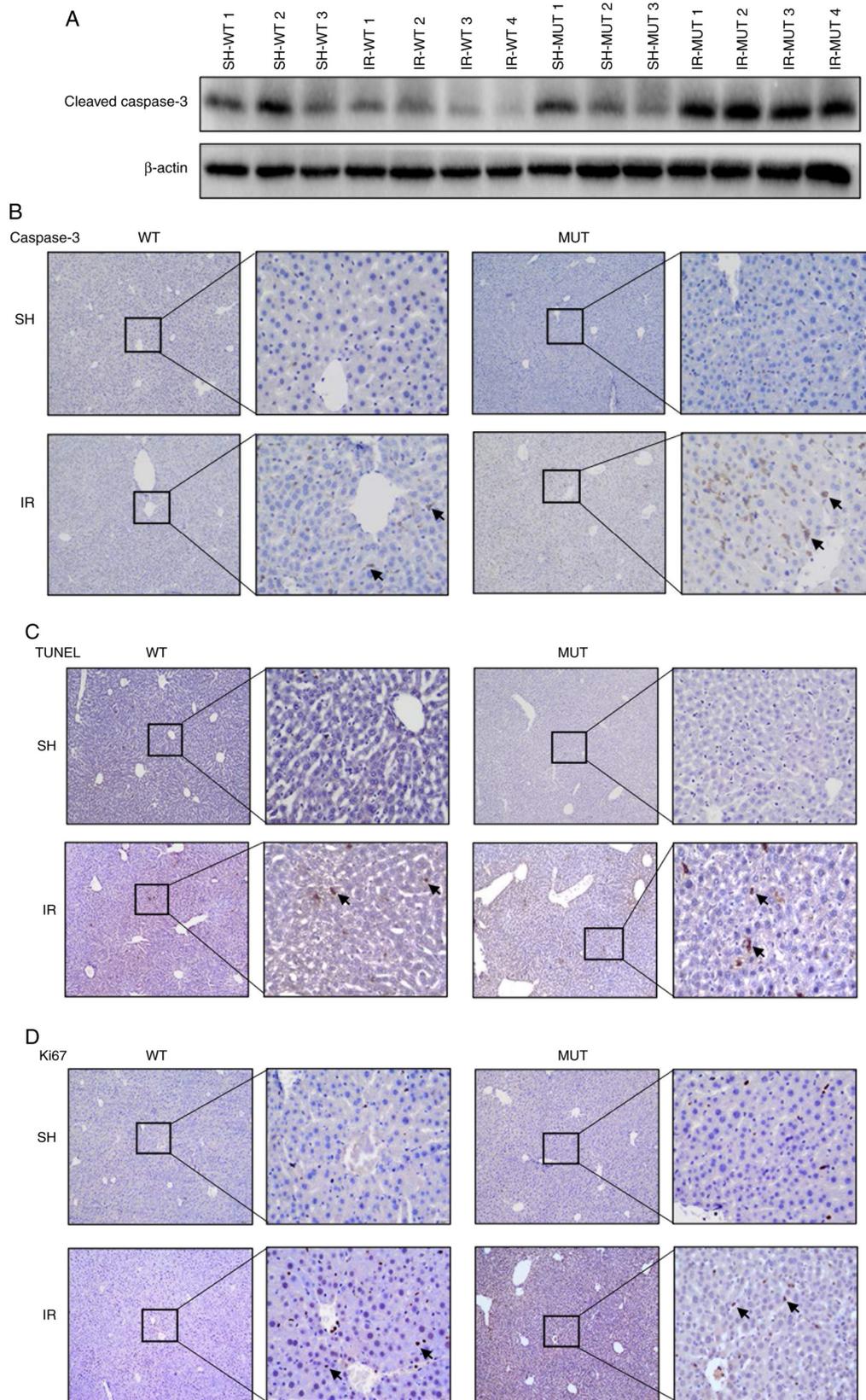
Figure 3. Apoptosis is increased in Smad3$^{-/-}$ mice following hepatic IR injury. (A) Protein expression levels of cleaved caspase-3 were determined via western blot analysis. SH-WT1, SH-WT2 and SH-WT3 indicate three randomly selected samples from the SH-WT group. IR-WT1, IR-WT2, IR-WT3 and IR-WT4 indicate three randomly selected samples from the IR-WT group. SH-MUT1, SH-MUT2 and SH-MUT3 indicate three randomly selected samples from the SH-WT group. IR-MUT1, IR-MUT2, IR-MUT3 and IR-MUT4 indicate three randomly selected samples from the IR-WT group. (B) Caspase-3 staining analysis in hepatic tissue from WT and Smad3 MUT mice. The positive cells are colored brown (black arrows; magnification, x100 and x400). (C) TUNEL staining indicated liver cell apoptosis in WT and Smad3 MUT mice. The positive cells are colored brown (black arrows; magnification, x100 and x400). (D) Ki67 staining analysis in hepatic tissue of WT and Smad3 MUT mice. The positive cells are colored brown (black arrows; magnification, x100 and x400). IR-WT, IR injury in Smad3 WT mice (n=10); SH-WT, sham-operated in Smad3 WT mice (n=10); IR-MUT, IR injury in Smad3 MUT mice (n=5); SH-MUT, sham-operated in Smad3 MUT mice (n=5). IR, ischemia-reperfusion; MUT, mutant; Smad3, SMAD family member 3; WT, wild-type.
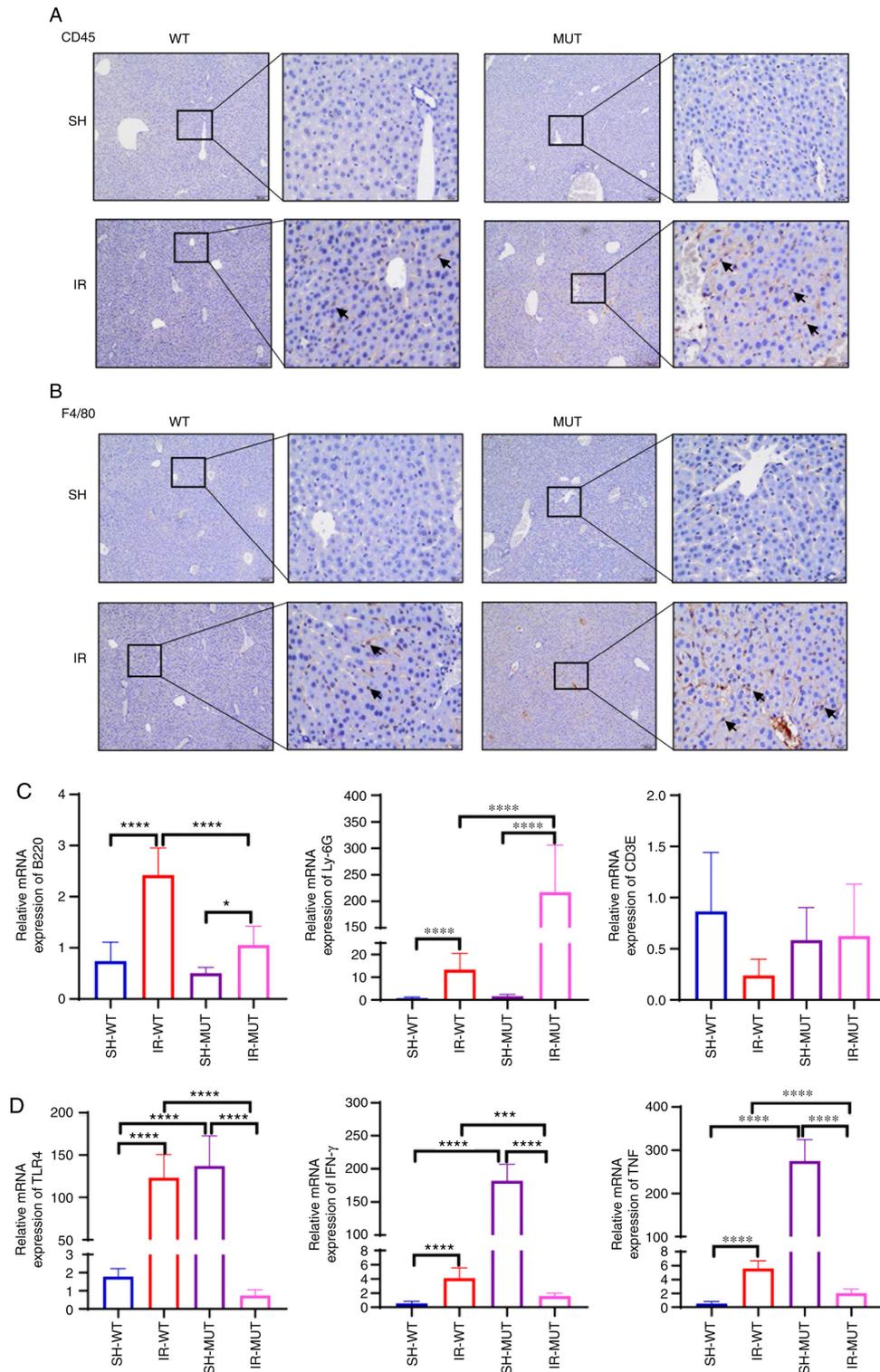
Figure 4. Inflammatory cell infiltration in Smad3^{-/-} mice following liver IR injury. (A) CD45 staining analysis in hepatic tissue from WT and Smad3 MUT mice. The positive cells are colored brown (black arrows; magnification, x100 and x400). (B) F4/80 staining analysis in hepatic tissue from WT and Smad3 MUT mice. The positive cells are colored brown (black arrows; magnification, x100 and x400). (C) B220, Ly-6G and CD3E mRNA expression levels were assessed in hepatic tissue homogenates via reverse transcription-quantitative PCR. The results of the relative mRNA expression levels of represent at least triplicate determinations. (D) mRNA expression levels of TLR4, IFN-γ and TNF were assessed in the liver tissues. The graph represents the relative mRNA expression levels from triplicate determinations. *P<0.05, ***P<0.001, ****P<0.0001. IR-WT, IR injury in Smad3 WT mice (n=10); SH-WT, sham-operated in Smad3 WT mice (n=10); IR-MUT, IR injury in Smad3 MUT mice (n=5); SH-MUT, sham-operated in Smad3 MUT mice (n=5). IR, ischemia-reperfusion; Ly-6G, lymphocyte antigen 6 complex locus G6D; MUT, mutant; Smad3, SMAD family member 3; TLR, Toll-like receptor; WT, wild-type.

that the TGF-β/Smad3 signaling pathway may have a protective role against hepatic IR injury in liver tissue. In order to further demonstrate the role of this pathway, it would be useful to interfere with the TGF-β/Smad3 signaling pathway using TGF-β neutralizing antibodies or inhibitors in future validation experiments.

TLR4 is an intermediary agent of inflammation and tissue damage in different IR damage models, such as hepatic (43), renal (44) and pulmonary (45) models. The activated TLR4 signaling pathway can promote an increase in the secretion of TNF-α, IFN-β and other inflammatory cytokines, thus causing increased blood reperfusion injury (46). A previous study observed increased TLR4 mRNA expression in Smad3$^{-/-}$ mice, and found that TLR4 was associated with lipopolysaccharide (LPS) hyperresponsiveness, leading to the increased expression of inflammatory cytokines (47). Therefore, the changes in the expression of TLR4 and other inflammatory cytokines, such as TNF and IFN-γ, in Smad3$^{+/+}$ mice after hepatic IR injury in the present study supported the aforementioned conclusions. In addition, in the sham operated group, the expression levels of TLR4, TNF and IFN-γ mRNA were significantly increased in Smad3$^{-/-}$ mice compared with in the Smad3$^{+/+}$. These results indicated that the TGF-β/Smad3 signaling pathway acts as an immunosuppressive factor that has a direct or indirect negative regulatory effect on the TLR4 signaling pathway, and loss of the TGF-β/Smad3 signaling pathway can promote TLR4-mediated inflammatory injury. Significant increases in the expression of TLR4, TNF and IFN-γ inflammatory cytokine genes were observed in Smad3$^{-/-}$ mice, indicating that endogenous deletion of the Smad3 gene in mice can lead to hyperreactivity of LPS *in vivo*, which can increase the secretion of inflammatory cytokines and hyperendotoxemia. In addition, mRNA expression levels of TLR4, TNF and IFN-γ were significantly downregulated in Smad3$^{-/-}$ mice after IR injury. It was suggested that Smad3$^{-/-}$ mice were resistant to IR injury and the associated endotoxic shock, resulting in an immune non-response, which may be associated with the loss of the TGF-β/Smad3 signaling pathway and persistently high LPS responses. Although the underlying mechanism between TGF-β/Smad3 signaling and TLR4 signaling is unclear, it is clear that the loss of the negative regulatory effects of TGF-β/Smad3, through either environmental or endogenous stimuli, can trigger the activation of TLR4 and downstream elements, and lead to an imbalance in the number of inflammatory cells.

In conclusion, the present study demonstrated that the TGF-β/Smad3 signaling pathway could protect against IR injury-induced damage in liver tissue repair and immune response. However, whether exogenous intervention treatment can reduce IR injury in the early stages of disease still needs further clarification, which provides a novel research direction for the prevention of IR injury.

Acknowledgements

Not applicable.

Funding

Availability of data and materials

The datasets used and/or analyzed during the present study are available from the corresponding author on reasonable request.

Authors' contributions

HL and XS conceived and performed the experiments, analyzed the data, prepared the figures, authored or reviewed drafts of the paper, and approved the final draft. YTo, TJ and XS conceived and directed the experiments, and reviewed and approved the final draft. YTo, TJ and XS confirm the authenticity of all the raw data. XL designed and guided the project research, and examined and approved the final manuscripts. YF and YTa conducted the experiments, reviewed and modified drafts of the paper, and approved the final draft. JY, TQ and RM performed the animal experiments, and approved the final draft. All authors read and approved the final manuscript.

Ethics approval and consent to participate

All animal experiments included in this protocol adhere to the Animal Research: Reporting *In Vivo* Experiments guidelines, and have been approved by the Animal Testing Ethics Committee of Sir Run Run Shaw Hospital, Zhejiang University School of Medicine (approval no. 20171120-14; Hangzhou, China).

Patient consent for publication

Not applicable.

Competing interests

The authors declare that they have no competing interests.

References

1. Takasu C, Vaziri ND, Li S, Robles L, Vo K, Takasu M, Pham C, Farzaneh SH, Shimada M, Stamos MJ, *et al*: Treatment with dimethyl fumarate ameliorates liver ischemia/reperfusion injury. World J Gastroenterol 23: 4508-4516, 2017.
2. Peralta C, Jiménez-Castro MB and Gracia-Sancho J: Hepatic ischemia and reperfusion injury: Effects on the liver sinusoidal milieu. J Hepatol 59: 1094-1106, 2013.
3. Shen XD, Ke B, Zhai Y, Amersi F, Gao F, Anselmo DM, Busuttil RW and Kupiec-Weglinski JW: CD154-CD40 T-cell costimulation pathway is required in the mechanism of hepatic ischemia/reperfusion injury, and its blockade facilitates and depends on heme oxygenase-1 mediated cytoprotection. Transplantation 74: 315-319, 2002.
4. Zabala V, Boylan JM, Thevenot P, Frank A, Senthoor D, Iyengar V, Kim H, Cohen A, Gruppuso PA and Sanders JA: Transcriptional changes during hepatic ischemia-reperfusion in the rat. PLoS One 14: e0227038, 2019.
5. Suzuki E, Ochiai-Shino H, Aoki H, Onodera S, Saito A, Saito A and Azuma T: Akt activation is required for TGF-β1-induced osteoblast differentiation of MC3T3-E1 pre-osteoblasts. PLoS One 9: e112566, 2014.
6. Derynck R and Budi EH: Specificity, versatility, and control of TGF-β family signaling. Sci Signal 12: eaav5183, 2019.
7. Brown KA, Pietenpol JA and Moses HL: A tale of two proteins: Differential roles and regulation of Smad2 and Smad3 in TGF-beta signaling. J Cell Biochem 101: 9-33, 2007.
8. Zou GL, Zuo S, Lu S, Hu RH, Lu YY, Yang J, Deng KS, Wu YT, Mu M, Zhu JJ, *et al*: Bone morphogenetic protein-7 represses hepatic stellate cell activation and liver fibrosis via regulation of TGF-β/Smad signaling pathway. World J Gastroenterol 25: 4222-4234, 2019.
9. Inagaki Y and Okazaki I: Emerging insights into Transforming growth factor beta Smad signal in hepatic fibrogenesis. Gut 56: 284-292, 2007.
10. Li T, Zhao S, Song B, Wei Z, Lu G, Zhou J and Huo T: Effects of transforming growth factor β-1 infected human bone marrow mesenchymal stem cells on high- and low-metastatic potential hepatocellular carcinoma. Eur J Med Res 20: 56, 2015.

11. Porowski D, Wirkowska A, Hryniewiecka E, Wyzgał J, Pacholczyk M and Pączek L: Liver Failure Impairs the Intrahepatic Elimination of Interleukin-6, Tumor Necrosis Factor-Alpha, Hepatocyte Growth Factor, and Transforming Growth Factor-Beta. BioMed Res Int 2015: 934065, 2015.

12. Wang RQ, Mi HM, Li H, Zhao SX, Jia YH and Nan YM: Modulation of IKKβ/NF-κB and TGF-β1/Smad via Fuzheng Huayu recipe involves in prevention of nutritional steatohepatitis and fibrosis in mice. Iran J Basic Med Sci 18: 404-411, 2015.

13. Park SO, Kumar M and Gupta S: TGF-β and iron differently alter HBV replication in human hepatocytes through TGF-β/BMP signaling and cellular microRNA expression. PLoS One 7: e39276, 2012.

14. Akhmetshina A, Palumbo K, Dees C, Bergmann C, Venalis P, Zerr P, Horn A, Kireva T, Beyer C, Zwerina J, et al: Activation of canonical Wnt signalling is required for TGF-β-mediated fibrosis. Nat Commun 3: 735, 2012.

15. Feng XH and Derynck R: Specificity and versatility in tgf-beta signaling through Smads. Annu Rev Cell Dev Biol 21: 659-693, 2005.

16. Ooshima A, Park J and Kim SJ: Phosphorylation status at Smad3 linker region modulates transforming growth factor-β-induced epithelial-mesenchymal transition and cancer progression. Cancer Sci 110: 481-488, 2019.

17. Liu ZY, Pan HW, Cao Y, Zheng J, Zhang Y, Tang Y, He J, Hu YJ, Wang CL, Zou QC, et al: Downregulated microRNA-330 suppresses left ventricular remodeling via the TGF-β1/Smad3 signaling pathway by targeting SRY in mice with myocardial ischemia-reperfusion injury. J Cell Physiol 234: 11440-11450, 2019.

18. Liu FF, Liu CY, Li XP, Zheng SZ, Li QQ, Liu Q and Song L: Neuroprotective effects of SMADs in a rat model of cerebral ischemia/reperfusion. Neural Regen Res 10: 438-444, 2015.

19. Percie du Sert N, Ahluwalia A, Alam S, Avey MT, Baker M, Browne WJ, Clark A, Cuthill IC, Dirnagl U, Emerson M, et al: Reporting animal research: Explanation and elaboration for the ARRIVE guidelines 2.0. PLoS Biol 18: e3000411, 2020.

20. Liu Y, Lu T, Zhang C, Xu J, Xue Z, Busuttil RW, Xu N, Xia Q, Kupiec-Weglinski JW and Ji H: Activation of YAP attenuates hepatic damage and fibrosis in liver ischemia-reperfusion injury. J Hepatol 71: 719-730, 2019.

21. Malý O, Zajak J, Hyšpler R, Turek Z, Astapenko D, Jun D, Váňová N, Kohout A, Radochová V, Kotek J, et al: Inhalation of molecular hydrogen prevents ischemia-reperfusion liver damage during major liver resection. Ann Transl Med 7: 774, 2019.

22. Livak KJ and Schmittgen TD: Analysis of relative gene expression data using real-time quantitative PCR and the 2(-Delta Delta C(T)) Method. Methods 25: 402-408, 2001.

23. Han L, Wang JN, Cao XQ, Sun CX and Du X: An-te-xiao capsule inhibits tumor growth in non-small cell lung cancer by targeting angiogenesis. Biomed Pharmacother 108: 941-951, 2018.

24. Yang X, Letterio JJ, Lechleider RJ, Chen L, Hayman R, Gu H, Roberts AB and Deng C: Targeted disruption of SMAD3 results in impaired mucosal immunity and diminished T cell responsiveness to TGF-beta. EMBO J 18: 1280-1291, 1999.

25. Bravatà V, Cammarata FP, Minafra L, Pisciotta P, Scazzone C, Manti L, Savoca G, Petringa G, Cirrone GAP, Cuttone G, et al: Proton-irradiated breast cells: Molecular points of view. J Radiat Res (Tokyo) 60: 451-465, 2019.

26. Zhai Y, Petrowsky H, Hong JC, Busuttil RW and Kupiec-Weglinski JW: Ischaemia-reperfusion injury in liver transplantation--from bench to bedside. Nat Rev Gastroenterol Hepatol 10: 79-89, 2013.

27. Jiménez-Castro MB, Cornide-Petronio ME, Gracia-Sancho J and Peralta C: Inflammasome-Mediated Inflammation in Liver Ischemia-Reperfusion Injury. Cells 8: E1131, 2019.

28. Lee PY, Wang JX, Parisini E, Dascher CC and Nigrovic PA: Ly6 family proteins in neutrophil biology. J Leukoc Biol 94: 585-594, 2013.

29. Xiang S, Chen K, Xu L, Wang T and Guo C: Bergenin Exerts Hepatoprotective Effects by Inhibiting the Release of Inflammatory Factors, Apoptosis and Autophagy via the PPAR-γ Pathway. Drug Des Devel Ther 14: 129-143, 2020.

30. Palomino-Schätzlein M, Simó R, Hernández C, Ciudin A, Mateos-Gregorio P, Hernández-Mijares A, Pineda-Lucena A and Herance JR: Metabolic fingerprint of insulin resistance in human polymorphonuclear leucocytes. PLoS One 13: e0199351, 2018.

31. Cutrn JC, Perrelli MG, Cavalieri B, Peralta C, Rosell Catafau J and Poli G: Microvascular dysfunction induced by reperfusion injury and protective effect of ischemic preconditioning. Free Radic Biol Med 33: 1200-1208, 2002.

32. Bielecka-Dabrowa A, Gluba-Brzózka A, Michalska-Kasiczak M, Misztal M, Rysz J and Banach M: The multi-biomarker approach for heart failure in patients with hypertension. Int J Mol Sci 16: 10715-10733, 2015.

33. Zhang G, Ge M, Han Z, Wang S, Yin J, Peng L, Xu F, Zhang Q, Dai Z, Xie L, et al: Wnt/β-catenin signaling pathway contributes to isoflurane postconditioning against cerebral ischemia-reperfusion injury and is possibly related to the transforming growth factorβ1/Smad3 signaling pathway. Biomed Pharmacother 110: 420-430, 2019.

34. Shang J, Sun S, Zhang L, Hao F and Zhang D: miR-211 alleviates ischaemia/reperfusion-induced kidney injury by targeting TGFβR2/TGF-β/SMAD3 pathway. Bioengineered 11: 547-557, 2020.

35. Wang S, Yin J, Ge M, Dai Z, Li Y, Si J, Ma K, Li L and Yao S: Transforming growth-beta 1 contributes to isoflurane postconditioning against cerebral ischemia-reperfusion injury by regulating the c-Jun N-terminal kinase signaling pathway. Biomed Pharmacother 78: 280-290, 2016.

36. Yang T, Zhang X, Ma C and Chen Y: TGF-β/Smad3 pathway enhances the cardio-protection of S1R/SIPR1 in in vitro ischemia-reperfusion myocardial cell model. Exp Ther Med 16: 178-184, 2018.

37. Larsson J, Goumans MJ, Sjöstrand LJ, van Rooijen MA, Ward D, Levéen P, Xu X, ten Dijke P, Mummery CL and Karlsson S: Abnormal angiogenesis but intact hematopoietic potential in TGF-beta type I receptor-deficient mice. EMBO J 20: 1663-1673, 2001.

38. Vander Ark A, Cao J and Li X: TGF-β receptors: In and beyond TGF-β signaling. Cell Signal 52: 112-120, 2018.

39. Schepers D, Tortora G, Morisaki H, MacCarrick G, Lindsay M, Liang D, Mehta SG, Hague J, Verhagen J, van de Laar I, et al: A mutation update on the LDS-associated genes TGFB2/3 and SMAD2/3. Hum Mutat 39: 621-634, 2018.

40. Waldrip WR, Bikoff EK, Hoodless PA, Wrana JL and Robertson EJ: Smad2 signaling in extraembryonic tissues determines anterior-posterior polarity of the early mouse embryo. Cell 92: 797-808, 1998.

41. Stewart AG, Thomas B and Koff J: TGF-β: Master regulator of inflammation and fibrosis. Respirology 23: 1096-1097, 2018.

42. Goumans MJ and Mummery C: Functional analysis of the TGFbeta receptor/Smad pathway through gene ablation in mice. Int J Dev Biol 44: 253-265, 2000.

43. Taylor KR, Trowbridge JM, Rudisill JA, Termeer CC, Simon JC and Gallo RL: Hyaluronan fragments stimulate endothelial recognition of injury through TLR4. J Biol Chem 279: 17079-17084, 2004.

44. Wu H, Chen G, Wyburn KR, Yin J, Bertolino P, Eris JM, Alexander SI, Sharland AF and Chadban SJ: TLR4 activation mediates kidney ischemia/reperfusion injury. J Clin Invest 117: 2847-2859, 2007.

45. Imai Y, Kuba K, Neely GG, Yaghubian-Malhami R, Perkmann T, van Loo G, Ermolaeva M, Veldhuizen R, Leung YH, Wang H, et al: Identification of oxidative stress and Toll-like receptor 4 signaling as a key pathway of acute lung injury. Cell 133: 235-249, 2008.

46. Liu Q and Zhang Y: PRDX1 enhances cerebral ischemia-reperfusion injury through activation of TLR4-regulated inflammation and apoptosis. Biochem Biophys Res Commun 519: 453-461, 2019.

47. McCartney-Francis N, Jin W and Wahl SM: Aberrant Toll receptor expression and endotoxin hypersensitivity in mice lacking a functional TGF-beta 1 signaling pathway. J Immunol 172: 3814-3821, 2004.